

**HEAT DISSIPATION ENHANCEMENT USING
GRAPHENE HEAT SINK**

WONG JER JIAN

UNIVERSITI SAINS MALAYSIA

2021

HEAT DISSIPATION ENHANCEMENT USING GRAPHENE HEAT SINK

By:

WONG JER JIAN

(Matric no: 137868)

Supervisor:

Dr Yu Kok Hwa

2nd July 2021

The dissertation is submitted to
Universiti Sains Malaysia

As partial fulfilment of the requirement to graduate with honors degree in
BACHELOR OF ENGINEERING (MECHANICAL ENGINEERING)



School of Mechanical Engineering
Engineering Campus
Universiti Sains Malaysia

DECLARATION

I hereby declare that this project entitled “Heat Dissipation Enhancement Using Graphene Heat Sink” submitted to Universiti Sains Malaysia is based on my original work except for quotations and citations which have been duly noted by explicit references.

Name: Wong Jer Jian

Date: 2nd July 2021

ACKNOWLEDGEMENT

First of all, I would like to express my gratitude to my supervisor, Dr. Yu Kok Hwa for his knowledge sharing and guidance throughout the research. Dr. Yu is helpful and knowledgeable. In terms of technical support, he had provided a workstation for me to complete the research. Besides, he also giving me advice on simulation settings and having discussion with me frequently. It is a great honor to complete the research under his supervision.

Furthermore, I would like to thank Dr. Muhammad Fauzinizam Bin Razali for organizing multiple workshops to guide students on project management and writing a good thesis. Other than that, I would like to thank the lecturers and librarians especially Madam Jamilah Hassan Basri, senior librarian at Universiti Sains Malaysia for sharing the thesis formatting and template.

Lastly, I would like to express my sincere gratitude to my family members and friends who support me mentally and financially. Their supports are essential and helped me in keeping up with the challenges faced prior to the completion of this research work. Thank you.

TABLE OF CONTENTS

DECLARATION	ii
ACKNOWLEDGEMENT	iii
TABLE OF CONTENTS	iv
LIST OF TABLES	vi
LIST OF FIGURES	viii
LIST OF SYMBOLS	x
ABSTRAK	xii
ABSTRACT	xiii
CHAPTER 1 Introduction	1
1.1 General introduction.....	1
1.2 Problem statement	3
1.3 Objective	3
1.4 Scope of project.....	4
1.5 Thesis outline	5
CHAPTER 2 Literature Review	6
2.1 Discovery and development of graphene	6
2.2 Factors affecting on the performance of heat sink	8
2.2.1 Surface finish of heat sink.....	8
2.2.2 Perforation and its shape on the heat sink fin.....	9
2.2.3 Geometry and shape of the fin of heat sink.....	12
CHAPTER 3 Methodology	16
3.1 Model geometry description.....	16
3.2 Numerical methods	18
3.2.1 Governing equations	18
3.2.1(a) Continuity equation	18

3.2.1(b)	Momentum equation.....	19
3.2.1(c)	Energy equation.....	19
3.2.2	Boundary conditions and setup in simulation.....	20
3.2.2(a)	Variation of heat flux applied.....	22
3.2.2(b)	Variation of fin height.....	22
3.2.3	Baseline case validation.....	22
3.3	Grid independence test.....	27
3.4	Calculation procedure.....	29
CHAPTER 4 Results and Discussion.....		31
4.1	Performance of plate fin heat sink under various mass flow rate of inlet air.....	31
4.2	Performance of plate fin heat sink under various heat fluxes.....	40
4.3	Fin efficiency of the heat sink under various fin height.....	48
CHAPTER 5 Conclusion and Future Recommendations.....		51
5.1	Conclusion.....	51
5.2	Recommendations for future work.....	52
REFERENCES.....		53

Appendices

LIST OF TABLES

		Page
Table 3.1	Different mass flow rates and corresponding Reynolds numbers studied.	21
Table 3.2	Thermophysical properties of working fluid and materials.	21
Table 3.3	Comparison of pressure drop with experimental results from Kim et al. [28] and numerical results from Mostafa et al. [27].	24
Table 3.4	Comparison of thermal resistance with experimental results from Kim et al. [28] and numerical results from Mostafa et al. [27].	25
Table 3.5	Results of grid independence test (base temperature).	27
Table 3.6	Results of grid independence test (thermal resistance).	27
Table 3.7	Results of grid independence test (pressure drop).	27
Table 4.1	Base temperature, outlet air temperature and average temperature of air for different flow rates.	32
Table 4.2	Heat transfer rate, thermal resistance, average heat transfer coefficient and average Nusselt number for different flow rates.	32
Table 4.3	Percentage difference of thermal resistance between materials with various flow rate.	37
Table 4.4	Pressure drop and pumping power required for different flow rates.	38
Table 4.5	Base temperature, outlet air temperature and average temperature of air for different input heat fluxes applied.	41
Table 4.6	Heat transfer rate, thermal resistance, average heat transfer coefficient and average Nusselt number for different heat fluxes applied.	41
Table 4.7	Percentage difference of thermal resistance between materials with various heat fluxes.	46

Table 4.8 Fin efficiency of heat sink with various fin heights.....48

LIST OF FIGURES

	Page
Figure 2.1	The configuration of heat sinks in the study [21]. 10
Figure 2.2	CAD model of novel plate fin heat sinks [22]. 11
Figure 2.3	Geometrical model in the study [23]. 12
Figure 2.4	Flared-fin heat sink [24]. 13
Figure 2.5	(a) Schematic and (b) geometrical configuration of rippling fin. 14
Figure 2.6	Configuration of heat sink with fin displacement. 15
Figure 3.1	Geometry of plate fin heat sink [23]. 17
Figure 3.2	Front view of the heat sink with fin height of 25 mm. 17
Figure 3.3	Flow direction of the air 21
Figure 3.4	Comparison of pressure drop with experimental results from Kim et al. [28] and numerical results from Mostafa et al. [27]. 24
Figure 3.5	Comparison of thermal resistance with experimental results from Kim et al. [28] and numerical results from Mostafa et al. [27]. 25
Figure 3.6	Temperature distribution contour plot from Hussain et al. [23]. 26
Figure 3.7	Temperature distribution contour plot from current simulation. 26
Figure 3.8	Mesh generated for the computational model. 28
Figure 4.1	Temperature contour plot of the heat sink (a) aluminium alloy 6061 (b) copper and (c) graphene at flow rate of 0.003925 kg/s. 34
Figure 4.2	Base temperature vs mass flow rate of inlet air. 35
Figure 4.3	Thermal resistance vs mass flow rate of inlet air. 36
Figure 4.4	Average Nusselt number vs mass flow rate of inlet air. 36
Figure 4.5	Pressure drop vs mass flow rate of inlet air. 39
Figure 4.6	Pumping power required vs mass flow rate of inlet air. 39

Figure 4.7	Temperature contour plot of the heat sink (a) aluminium alloy 6061 (b) copper and (c) graphene at heat flux of 25000 W/m^2	43
Figure 4.8	Base temperature of heat sink vs input heat flux.	44
Figure 4.9	Thermal resistance of heat sink vs input heat flux.....	44
Figure 4.10	Average Nusselt number vs input heat flux.	45
Figure 4.11	Pumping power vs heat flux applied.....	47
Figure 4.12	Fin efficiency of heat sink with various fin heights.....	49

LIST OF SYMBOLS

A	Area section of the inlet (m^2)
A_T	Total area of the heat sink subjected to the fluid flow (m^2)
A_{base}	Area of the base of the heat sink
B	Base height (m)
C_p	Specific heat capacity (J/kgK)
C_{pa}	Specific heat capacity of air at average temperature (J/kgK)
D_h	Hydraulic diameter of inlet (m)
\bar{h}	Average heat transfer coefficient
H	Fin height (m)
k	Thermal conductivity (W/mK)
k_a	Thermal conductivity of air at average temperature (W/mK)
L	Length of the heat sink (m)
L_c	Corrected length (m)
\dot{m}_a	Mass flow rate of air (kg/s)
N_f	Number of fins
\overline{Nu}	Average Nusselt number
P	Pressure (Pa)
P_{in}	Inlet pressure (Pa)
P_{out}	Outlet pressure (Pa)
P_{pump}	Pumping power (W)
ΔP	Pressure drop between inlet and outlet (Pa)
P_w	Wetted perimeter of inlet (m)
q	Heat flux (W/m^2)
Q	Heat transfer rate (W)
Re_{Dh}	Reynold number

R_{th}	Thermal Resistance (K/W)
t	Thickness of fin (m)
T	Temperature (K)
T_{avr}	Average air temperature (K)
T_b	Base temperature (K)
T_{in}	Inlet temperature of air (K)
T_{out}	Outlet temperature of air (K)
\vec{U}	Velocity (m/s)
U_{avr}	Average velocity of air (m/s)
u	Velocity components in x-direction (m/s)
v	Velocity components in y-direction (m/s)
w	Velocity components in z-direction (m/s)
W	Width of heat sink (m)
τ	Viscous stress tensor (Pa)
\emptyset	Dissipation term
μ	Dynamic viscosity of air (kg/ms)
η_{fin}	Fin efficiency
ρ	Density (kg/m ³)
ρ_a	Density of air (kg/m ³)

ABSTRAK

Pelepasan haba merupakan salah satu cabaran yang perlu diatasi untuk meningkatkan prestasi komponen elektronik. Dalam kajian ini, penyelidikan berangka mengenai penggunaan grafin dalam sink haba telah dijalankan dan prestasi termanya telah dikaji dan dibanding dengan sink haba yang diperbuat daripada tembaga dan aloi aluminium. Khususnya, kesan ketinggian sirip, fluks haba input dan kadar aliran udara pada prestasi terma sink haba telah dikaji dan didokumentasikan dalam tesis ini. Prestasi terma dinilai berdasarkan rintangan haba, purata nombor Nusselt, kuasa pam dan efisiensi sirip sink haba. Pengajian ini telah menunjukkan bahawa sink haba grafin yang mempunyai konduktiviti terma yang tinggi memberi terma rintangan yang paling rendah dan purata nombor Nusselt yang paling tinggi antara bahan lain. Bahan-bahan yang digunakan tidak menyumbang kepada perubahan kuasa pam yang diperlukan untuk pengaliran air. Konduktiviti terma grafin yang tinggi dapat meminimumkan penurunan efisiensi sirip yang disebabkan oleh peningkatan ketinggian sirip, peratusan penurunan efisiensi sirip tidak lebih daripada 2% dalam kajian ini.

ABSTRACT

Heat dissipation is one of the challenges that need to be tackled to enhance the performance of the electronic components. In current study, the numerical investigation on the use of graphene in designing a plate fin heat sink and evaluation of thermal performance by comparing with the conventional material (copper and aluminium alloy) are performed. In particular, the effects of fin height, heat flux and flow rate of the working fluid on the thermal performance of the heat sink are studied and documented in the thesis. The thermal performance is evaluated in terms of the thermal resistance, average Nusselt number, pumping power required and fin efficiency of the heat sink. This study has shown that the graphene heat sink which has a higher thermal conductivity yields the lowest thermal resistance and gives the highest average Nusselt number among other materials. The pumping power required for the flow of working fluid is independent to the material used. With its high intrinsic thermal conductivity, graphene heat sink reduced the drop in terms of fin efficiency when fin height is increased, the percentage of the fin efficiency drop with the height is not more than 2% in the study.

CHAPTER 1

Introduction

1.1 General introduction

The demand on electronic equipment is gradually increasing and the current trend is leading toward smaller size of the electronic devices and chips. The ongoing trend of miniaturization is leading to the development of electronic devices with the demand toward faster and more advanced application, thus making the characteristic dimension of the devices to become substantially smaller, from microscale into nanoscale [1]. However, these technological advances are causing the packaging power density of electronic components to continue in the increasing trend and leading to higher power consumption and heat flux generation for individual components and the assembly. Heat generated in the electronic device will result in build-up of thermal stress which eventually led to deteriorated performance, often followed by failures. These changes had made thermal management as a priority in controlling the operating temperature while enhancing the performance and reliability.

In fact, there are different kinds of heat dissipation device to remove this unwanted heat that released from the electronic device such as heat pipes, cold plate, heat sink, etc. Heat sink is the most common devices used for thermal management. It is usually made of metals with high thermal conductivity and low coefficient of thermal expansion in order to reduce the temperature difference between the chip and the fin. The conventional materials that are commonly used to build a heat sink are copper and aluminium alloy [2]. The heat transfer rate of the heat sink increases with thermal conductivity of metal, therefore copper which has a higher thermal conductivity has a better heat dissipation performance as compared with that of

aluminium alloy, but the disadvantage of this copper heat sink is their weight and cost [3].

Presently, graphene is deemed to be a promising material that can be practically used in electronic devices and circuits. Graphene is a material that composed of pure carbon, the chemical composition of graphene is similar to diamond and graphite, it is an allotrope of carbon which consists of carbon atoms that are sp^2 bonded into honeycomb lattice [4]. It is a high elasticity and hardness material; the thermal conductivity of graphene is high and capable of self-cooling and self-healing. These intrinsic characteristics made it an excellent alternative for advanced applications in future electronics. Among these unique properties of graphene, the high intrinsic thermal conductivity of graphene shows a great potential in tackling the thermal management challenge in electronic system. A study related to measurement of suspended graphene using optothermal Raman technique by Balandin et al. [5] showed that graphene has a thermal conductivity that greatly exceeding that of bulk graphite. The exceptional thermal properties of graphene motivated the research on the graphene derivatives, such as graphene thermal interface material, graphene oxide, graphene films, etc [6]. Other than materials, other criteria and parameters like arrangement of fins, geometric parameters need to be considered while designing a heat sink. For example, heat dissipation performance of the pin-fins in staggered arrangement is more efficient than inline arrangement, as turbulence effect around the pin fins increases with staggered arrangement, resulting in the significant increase of the cooling rate [7]. The design of a high-performance heat sink that can dissipate great amount of heat is important to tackle the heat generation issue brought by the high-power consumption miniaturized electronics.

1.2 Problem statement

Apart from the conventional materials, like copper and aluminium alloys, graphene is also a promising material that can be employed to enhance the heat dissipation performance from heat sink due to its relatively high thermal conductivity. It is a sheet of single-layered carbon atoms packed densely into a honeycomb crystal lattice that possesses high intrinsic thermal conductivity in which the thermal conductivity can reach a maximum of 5000 W/mK. The superior thermal properties make it a suitable choice in dissipating the heat from the electronic devices effectively. Besides, the performance of heat sink may influence by different parameters, such as its geometry, fin height, flow rate of air, etc. Therefore, numerical simulation study on the performance of heat sink under different parameters (i.e., mass flow rate of air, heat flux generated, material, fin height) is essential.

1.3 Objective

The objectives of this project are summarized as follows:

- To investigate the effects of high heat conductivity material on thermal performance of heat sink.
- To investigate the influences of flow rate of inlet air and heat flux for conventional heat sink and graphene heat sink.
- To explore and investigate the effects of fin height and materials on the fin efficiency of heat sink.

1.4 Scope of project

The project will be focusing on the numerical study on the performance of heat sink in heat dissipation with graphene, aluminium and copper, with the use of ANSYS Fluent software. Finite-volume method is employed to simulate the steady-state conjugate heat transfer of the heat sink, by solving the relevant governing equations stated in Chapter 3.2.1. In this study, the plate fin heat sink is subjected to impinging flow, and the air flow is assumed steady, turbulent and incompressible. The radiation and the effect of gravity acceleration are neglected. Three materials which include aluminium alloy 6061, copper and graphene are considered to be the materials of heat sink to compare and evaluate its thermal performance, and the performance is evaluated based on its thermal resistance, pressure drop of air, the average Nusselt number and fin efficiency. Besides, the thermal performance of the heat sink is evaluated with various parameters which include input heat flux, flow rate of air and fin height of the heat sink. Baseline cases are validated to ensure the accuracy of the numerical scheme used. Experimental work is not considered in this study.

1.5 Thesis outline

This thesis is structured into five chapters:

1. Chapter 1 began with a general introduction about the problems of thermal management of the electronic device and introduction of graphene.
2. Chapter 2 discussed the literature review on the development of graphene and factors that contributing to the heat dissipation performance of the heat sink.
3. Chapter 3 described and explained the methodology that implemented in the numerical simulation.
4. Chapter 4 showed the results obtained from the numerical simulation and discussed the performance of the heat sink.
5. Chapter 5 concluded the overall research and gave several recommendations for future work.

CHAPTER 2

Literature Review

2.1 Discovery and development of graphene

As the increase in demand on miniaturization of electronic components, one of the major challenges that required to be solved is the growing power consumptions in the electronic components. In the field of nanoelectronics among the electronic components, the typical material of heat sink is copper [8]. In order to further enhance the heat dissipation, a material with extremely high thermal conductivity is preferred [9].

An allotrope of carbon, graphene is experimentally discovered by Geim and Novoselov with mechanical exfoliation method in 2004 [10]. In this method, the graphite flakes are exfoliated from the bulk HOPG (Highly Ordered Pyrolytic Graphite) surface, flakes are then split repeatedly into thinner pieces with adhesive tape until the single layer of graphene is obtained [11]. Due to the unique structure of graphene, the single sheet of sp^2 bonded graphene, exhibits extraordinary mechanical, thermal and electrical properties [12]. Among all these properties, the high intrinsic thermal conductivity had attracted the attention of the research in recent year. The study of the thermal conductivity of suspended single-layer graphene which obtained from exfoliated method is first conducted experimentally by Balandin et al. [5] using Raman spectroscopy and reported that its thermal conductivity is fall in the range of 4840 W/mK to 5300 W/mK. Other than that, the thermal conductivity of suspended chemical vapor deposition (CVD) graphene is studied by Cai et al. [13] and reported that its thermal conductivity exceeded 2500 W/mK at 350 K and it was as high as 1400 W/mK at 500 K. In addition, other optothermal studies with suspended graphene

reported that the thermal conductivity of graphene is ranging from 1500 to 5000 W/mK [14].

With the extraordinary thermal conductivity of graphene, several studies have been conducted by the researchers on the development of the graphene derivatives to enhance the heat dissipation potential of heat dispersants. In recent years, the studies of heat dissipation enhancement with graphene nanosheets coating are proposed by different researchers. Jaafar et al. [15] who studied the effect of chemical spray graphene nanosheet coating on the performance of heatsink concluded that the high thermal conductivity, surface morphology and roughness of graphene material are the contributing factor for the improvement on the performance of heat sink in heat dissipation. The island shape graphene surface which due to substrate heating and annealing process had increased the surface area and enhanced the heat dissipation process. Besides, Chun et al. [16] who studied the effect of the use of multilayer graphene-coated surface on the copper subtraction in evaporation and conduction heat transfer concluded that the evaporation and conduction heat transfer can be enhanced with graphene-coated surface. Furthermore, the heat removal performance of the graphene-coated aluminium heat sink is studied by Hadi et al. [17] and found out that the graphene coated heat sink has a better thermal performance than a uncoated heat sink. He also believed that the graphene layer increases the surface area of heat transfer by roughening the surface texture. In short, graphene is suitable to be used in electronic cooling sector and bring a great enhancement in thermal management to the electronic components.

2.2 Factors affecting on the performance of heat sink

Other than the influence of the material that applied on the heat sink, the heat removal performance of the heat sink is also affected by other factors such as the geometry parameters of the heat sink, surface finish of the heat sink, velocity of the air flow, shape of perforation on fin and so forth.

2.2.1 Surface finish of heat sink

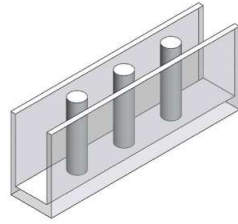
The surface finish of the heat sink has a significant effect on the performance of heat sink in heat dissipation. Generally, a rough surface finish improves the heat transfer performance, as the friction between the air and smooth surface is relatively less as compared with the friction between the air and rough surface. Oguntala et al. [18] conducted numerical investigation on the thermal behaviour and subsequent heat transfer augmentation of cylindrical micro-fins with artificial surface roughness on heat dissipation improvement of microprocessors. From his study, thermal performance of the device enhanced in the rough fins as compared with smooth fins, the temperature difference between the rough-micro-fin and the bulk temperature is increased by the increase in temperature uniformity in the rough fins. Other than that, the effect of artificial roughness manufactured by direct metal laser sintering (DMLS) to augment convective heat transfer in flat and finned heat sinks was assessed experimentally by Ventola et al. [19]. He observed that the average convective heat transfer on the rough flat and rough fin surfaces was improved by 63% and 35%, in comparison to a smooth surface. Both studies proved that surface finish is an important factor to enhance the heat transfer performance of heat sink.

2.2.2 Perforation and its shape on the heat sink fin

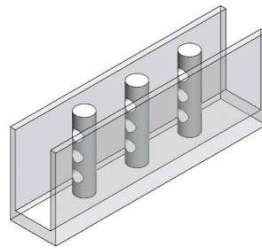
Inserting perforation on the fin of the heat sink is one of the good approaches to enhance the heat transfer of the heat sink. The perforation on the fin surfaces not only increase the surface area and improve the heat transfer rate, but also reduce the overall weight of the heat sink at the same time. Gupta et al. [20] conducted numerical investigation on the effect of perforation number and shape on the thermal performance of solid square micro-pin fin heat sink, the thermal performance is evaluated based on the ratio of Nusselt number and pressure drop in the study. Based on the results, he concluded that the pressure drop decreases while the Nusselt number increases with the increase of perforations number. For the case of pressure drop, he believed that the increase in number of perforations decrease the obstruction offered by the pins to air flow rate and thus yields lower pressure drop in the heat sink. For the case of Nusselt number, the increase in number of perforations increases the convective surface area, and results in further increases the thermal dissipation rate of the heat sink. He also claimed that the pressure drop for square perforations is lower and perform better in heat dissipation than the circular perforation because surface area and turbulence effect are increased at the sharp corners.

Instead of making perforation, the thermal performance of the heat sink can be further enhanced with by adding a splitter. Huang et al. [21] examined the effect of implementation of perforations and splitters on a pin fin on the performance of the heat sink. From his study, he found out that the added splitter behind the pin fin could descend the vortex intensity and spread the streamlines behind the pin fin. Besides, the implementation of perforation allows the air flow freely through the perforation and prevent the occurrence of vortex behind the pin. He concluded that these two effects

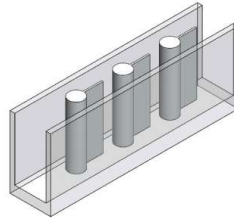
can be combined and further enhanced the thermal performance by utilizing perforation and splitter simultaneously.



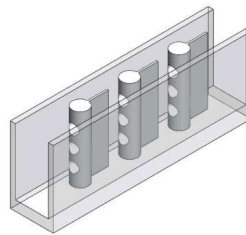
(a) Plate pin fin heat sink



(b) Plate pin fin heat sink with perforations



(c) Plate pin fin heat sink with splitters

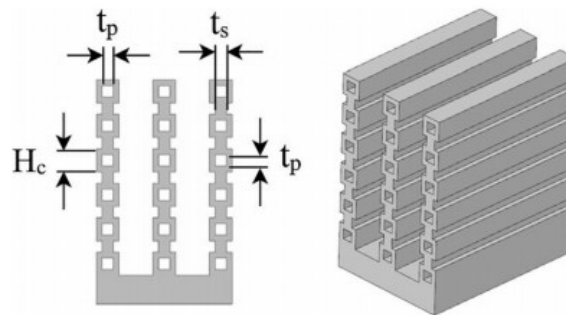


(d) Plate pin fin heat sink with splitters and perforations

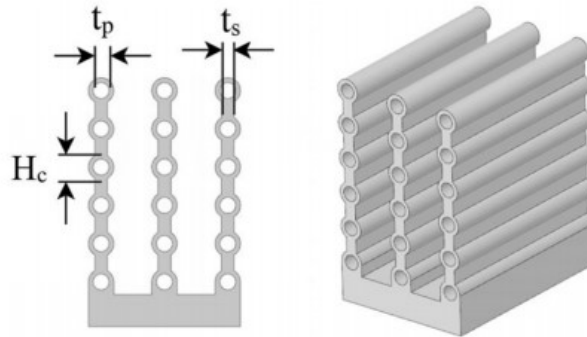
Figure 2.1 The configuration of heat sinks in the study [21].

Effects of perforations and slots in a plate-fin heat sink are studied by Tariq et al. [22]. He proposed two novel designs of heat sink with rectangular and circular-shaped perforations and slots, comparing their performance in heat dissipation with

plate-fin heat sink in the study. The results show that the convection coefficient is enhanced with the combination of perforations and slots, because perforation and slots increase the heat transfer area of heat sink. In addition, the pressure drop of the heat sink is also reduced with the slots and perforations, which results in reduction of the power required to overcome the pressure drop. Other than enhanced the heat transfer and pressure drop, the weight of the proposed design is also lower with the design of perforations and slots.



(a) Heat sink with rectangular-shaped perforation

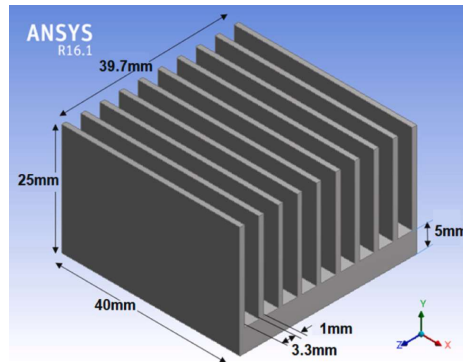


(a) Heat sink with circular-shaped perforation

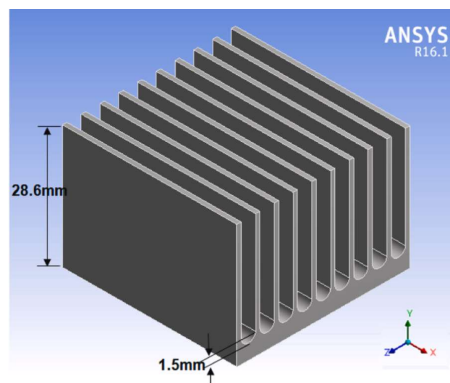
Figure 2.2 CAD model of novel plate fin heat sinks [22].

2.2.3 Geometry and shape of the fin of heat sink

Geometry of the heat sink also an important factor that might influence the heat dissipation of heat sink. The effect of fillet profile on the performance of heat sink subjected to parallel flow and impinging flow is studied by Hussain et al. [23] numerically. In this study, performance of heat sink is evaluated based on thermal resistance and base temperature of the heat sink. He concluded that fillet profile increases the heat transfer area, which results in promoting the heat dissipation from the hot region. The fillet profile also improves the heat distribution; thus the convection is smoothed near the bottom of the plate fin.



(a) Heat sink without fillet profile



(b) Heat sink with fillet profile

Figure 2.3 Geometrical model in the study [23].

Furthermore, a flared-fin heat sink design is proposed by Luo et al. [24] to satisfy the high-density heat dissipation of concentrating photovoltaic system. In the study, parameters such as fin height, number of fins, and inclination angle are varied to study their effect on the thermal performance of the heat sink. Based on the results, flared-fin heat sink is better in heat dissipation as compared with that of plate-fin heat sinks. With its exceptional geometric design, the heat is distributed evenly to the fins, which is favorable for promoting the convection heat transfer of the fins. Besides, thermal resistance of the heat sink is sensitive to the number of fins, great amount of heat can be removed with the increase of fins. However, increasing number of fins led to the reduction of the spacing between the adjacent fins which might obstruct the flow of the working fluid. He also concluded that the overall thermal resistance decreased nonlinearly with the increasing fin height, due to the increased of fin surface area.

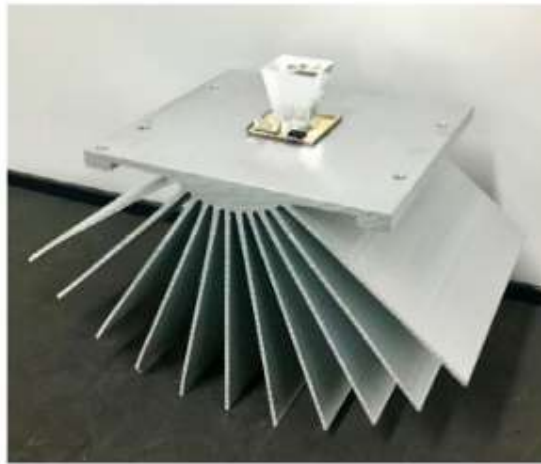
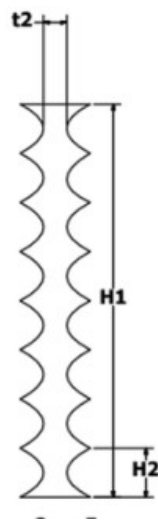


Figure 2.4 Flared-fin heat sink [24].

Ghandouri et al. [25] proposed a rippling fin shape to enhance the convective heat transfer in heat sinks and reduce the weight of heat sink. In the study, he concluded the cooling performance of heat sink is higher than a rectangular fin heat sink, because the ripples design forced the air towards the heated wall, created a mixture between the working fluid at the centerline of the flow and the hot wall, the boundary layer is interrupted and become thinner, which results in reducing the thermal resistance and enhance the heat dissipation rate of heat sink.



(a)



(b)

Figure 2.5 (a) Schematic and (b) geometrical configuration of rippling fin.

Fin displacement is one of the factors that contributing to the heat dissipation of heat sink. The effect of fin displacement on the thermal performance of rectangular fin heat sink is investigated by Abbas et al. [26]. He concluded that heat sink with fin displacement achieved a lower thermal resistance than a conventional rectangular fin heat sink, but this effect can be counteracted by the fin spacing. Fin displacement with low fin spacing enhances the thermal performance by slowing down the merging of boundary layers and decrease the length of fully developed region. Besides, low fin spacing also induces the ambient air into the fin array at the upper portion of the heat sink which further enhance cooling performance of the heat sink.

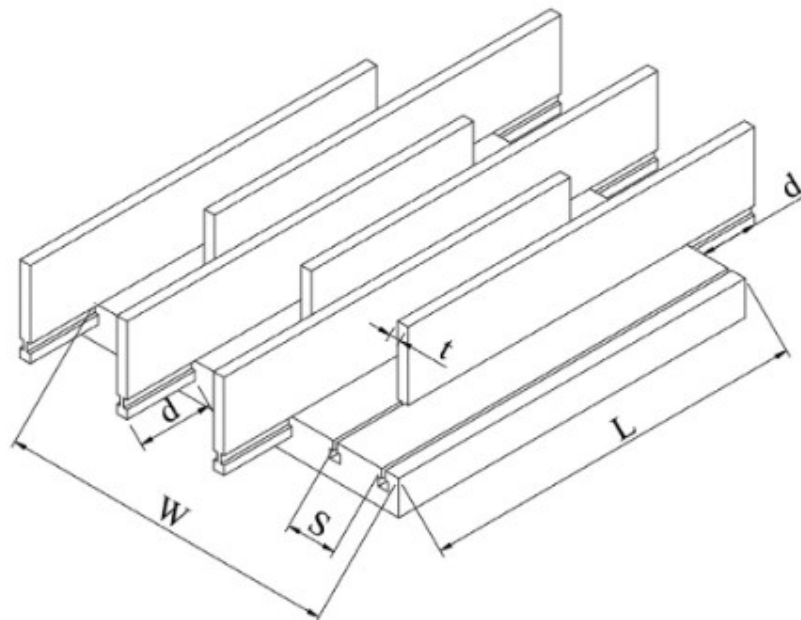


Figure 2.6 Configuration of heat sink with fin displacement.

CHAPTER 3

Methodology

3.1 Model geometry description

The physical geometry of the plate fin heat sink is built according to the geometry and dimensions stated by Mostafa et al. [27], as illustrated in Figure 3.1. The length and width of the base are 40 mm and 39.7 mm, respectively, with thickness of 5 mm. The thickness of fins and channel width are constant across the length of base and specified to be 1 mm and 3.3 mm, respectively. The height of the fins is 20 mm without considering the thickness of base. A fluid domain with dimension of 40 mm \times 39.7 mm \times 26 mm is built and enclosed the heat sink to study the conjugate heat transfer analysis. The plate fin heat sink in the study is subjected to impinging flow, in which the air impinges on the heat sink (inlet) along the y-axis and flow parallel to the two outlets along the x-axis.

For the study of fin efficiency, the height of the fin is increased from 20 mm to 50 mm with an increment of 5 mm. A front view of the geometry with fin of 25 mm is illustrated in Figure 3.2.

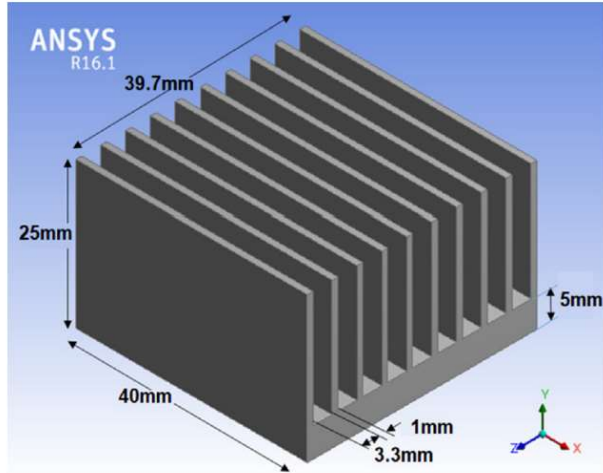


Figure 3.1 Geometry of plate fin heat sink [23].

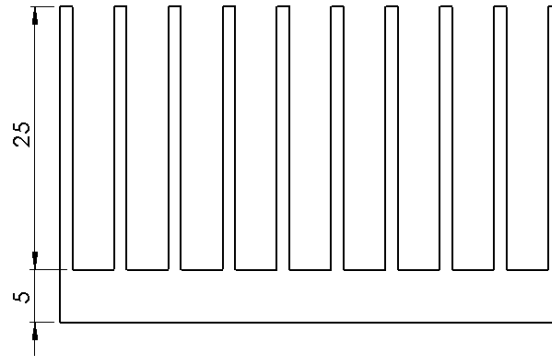


Figure 3.2 Front view of the heat sink with fin height of 25 mm.

3.2 Numerical methods

3.2.1 Governing equations

The simulations are set up in ANSYS Fluent 2019 and several assumptions are made in the simulation.

1. The air flow is steady, turbulent and incompressible.
2. Three-dimensional fluid-solid conjugate.
3. Effect of gravity acceleration is neglected.
4. Radiation effect is neglected.
5. Energy is conserved.
6. The thermophysical properties of the materials and air are shown as in Table 3.2.

The convective heat transfer characteristics are achieved by solving the governing equations as follow:

3.2.1(a) Continuity equation

The continuity equation is given by:

$$\nabla \cdot (\rho \vec{U}) = 0 \quad (3.1)$$

where ρ is the density of fluid, and \vec{U} is the velocity.

3.2.1(b) Momentum equation

The Navier-Stoke equations across the x , y and z directions are given as followings:

$$\nabla(\rho \vec{U}u) = -\frac{\partial P}{\partial x} + \frac{\partial \tau_{xx}}{\partial x} + \frac{\partial \tau_{yx}}{\partial y} + \frac{\partial \tau_{zx}}{\partial z} \quad (3.2)$$

$$\nabla(\rho \vec{U}v) = -\frac{\partial P}{\partial y} + \frac{\partial \tau_{xy}}{\partial x} + \frac{\partial \tau_{yy}}{\partial y} + \frac{\partial \tau_{zy}}{\partial z} \quad (3.3)$$

$$\nabla(\rho \vec{U}w) = -\frac{\partial P}{\partial z} + \frac{\partial \tau_{xz}}{\partial x} + \frac{\partial \tau_{yz}}{\partial y} + \frac{\partial \tau_{zz}}{\partial z} \quad (3.4)$$

where ρ is the density of fluid, \vec{U} is the velocity, (u , v and w) are velocity components in three directions, P is pressure and τ is the viscous stress tensor.

3.2.1(c) Energy equation

The energy equation is given by:

$$\nabla(\rho h \vec{U}) = -P \nabla \vec{U} + \nabla(k \nabla T) + \phi \quad (3.5)$$

where ρ is the density of fluid, \vec{U} is the velocity, h is the aggregate enthalpy, ϕ is the dissipation term, k is thermal conductivity and T is temperature.

3.2.2 Boundary conditions and setup in simulation

The boundary conditions are considered based on the experimental work of Kim et al. [28] and numerical study of Mostafa et al. [27]. According to the setup in the study, the air flows at inlet with four different Reynolds numbers ($Re = 1333, 2667, 4000$ and 5334) at 25°C . Based on the inlet condition and inlet hydraulic diameter with turbulence intensity of 5%, the corresponding flow rate is calculated with Equation (3.6) and tabulated in Table 3.1, while the inlet hydraulic diameter is calculated with Equation (3.7). As the heat sink is subjected to impinging flow, the air flows from the top of the heat sink along the y-axis and flow towards the two outlets along the x-axis.

$$Re_{Dh} = \frac{\rho U_{avr} D_h}{\mu} \quad (3.6)$$

where U_{avr} is the average velocity of air, ρ is the density of air, D_h is the inlet hydraulic diameter and μ is the dynamic viscosity of air.

$$D_h = \frac{4A}{P_w} \quad (3.7)$$

where A is the area section of the inlet and P_w is the wetted perimeter of the inlet.

According to Kim et al. [28], the heat sink is made of aluminium alloy 6061 with thermal conductivity of 171 W/mK . The bottom surface of heat sink is subjected to a uniform heat flux of 18750 W/m^2 . The thermophysical properties of the air, aluminium alloy, copper and graphene are shown in Table 3.1. The walls of the heat sink and the duct are assumed adiabatic walls in the simulation. No-slip condition is selected for both wall domains. For the pressure-velocity coupling, the coupled algorithm is applied, and second-order scheme is selected to solve the energy and momentum conservation equations. Besides, the Shear-Stress-Transport (*SST*) $K-\omega$

model is selected to carry out the numerical analysis [29]. The convergence criterion of 1×10^{-6} is set for the energy equation and 1×10^{-5} for the continuity equation.

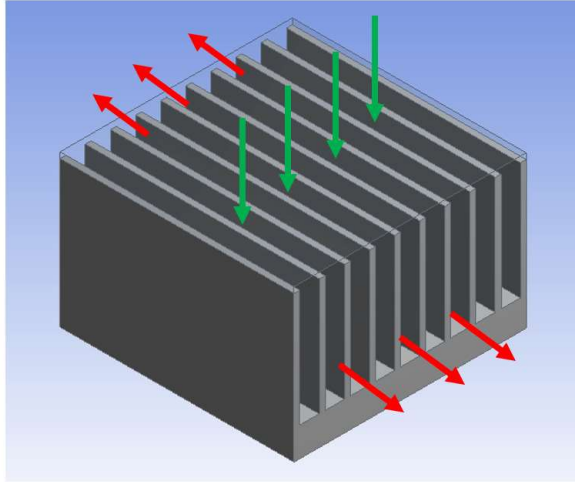


Figure 3.3 Flow direction of the air

Table 3.1 Different mass flow rates and corresponding Reynolds numbers studied.

No.	Corresponding Reynold Number, Re_{Dh}	Mass Flow Rate, \dot{m}_a (kg/s)
1	1333.63	0.000981
2	2667.26	0.001962
3	4000.89	0.002944
4	5334.52	0.003925

Table 3.2 Thermophysical properties of working fluid and materials.

Materials	Density, ρ (kg/m ³)	Specific heat capacity, C_p (J/kgK)	Thermal conductivity, k (W/mK)	Dynamic viscosity, μ (kg/ms)
Air [27][28]	1.1774	1005.7	0.02624	1.8462×10^{-5}
Aluminium Alloy 6061 [27][28]	2700	897	171	-
Copper [30]	8950	390	390	-
Graphene [31][32][33]	2267	700	3410	-

3.2.2(a) Variation of heat flux applied

To study the effect of heat flux to the performance of the heat sink, the boundary conditions stated above remain the same and the heat flux that subjected to the bottom surface of the heat sink is set to 10000 W/m^2 , 15000 W/m^2 , 20000 W/m^2 and 25000 W/m^2 , respectively.

3.2.2(b) Variation of fin height

To investigate the effect of fin height and materials on the fin efficiency of the heat sink, the setup of the simulation used is similar as stated in Chapter 3.2.2 and the height of the fin is set to 25 mm, 30 mm, 35 mm, 40 mm, 45 mm and 50 mm, respectively. Aluminium alloy and graphene with thermophysical properties stated in Table 3.2 is applied in the simulation.

3.2.3 Baseline case validation

Mostafa et al. [27] and Hussain et al. [23] were taken as the reference paper to validate and ensure the accuracy of the numerical scheme and model used. The assumptions and boundary conditions are implemented in the simulation are similar as stated in Chapter 3.2.2. On this basis, the pressure drop of air and overall thermal resistance of the aluminium alloy 6061 heat sink at various mass flow rates are compared with the experimental work of Kim et al. [28] and numerical simulation done by Mostafa et al. [27]. The results of pressure drop and overall thermal resistance from the paper was digitized with WebPlot Digitizer and the results are compared with the simulated results as tabulated in Table 3.3 and Table 3.4, and illustrated in Figure 3.4 and Figure 3.5, respectively.

According to the Mostafa et al. [27], thermal resistance of the heat sink is calculated by Equation (3.8).

$$R_{th} = \frac{1}{\bar{h}A_T} \quad (3.8)$$

where A_T is the total area of the heat sink subjected to the fluid flow and \bar{h} is the average heat transfer coefficient.

Calculation of total area of the heat sink subjected to the fluid flow and average heat transfer coefficient is done by using Equation (3.9) and (3.10), respectively.

$$A_T = WL + 2H(L(N_f - 1) + tN_f) + 2BW \quad (3.9)$$

$$\bar{h} = \frac{Q}{A_T(T_b - T_{avr})} \quad (3.10)$$

where W and L are the width and length of the heat sink, respectively, N_f , B , H and t are the number of fins, base height, fin height above the base and thickness of the fin respectively. While Q is the heat transfer rate calculated by Equation (3.11), T_b is the fin base temperature and T_{avr} is the average air temperature given by Equation (3.12).

$$Q = qA_{base} \quad (3.11)$$

$$T_{avr} = \frac{(T_{out} + T_{in})}{2} \quad (3.12)$$

where q is the heat flux applied, A_{base} is the area of the base, T_{avr} is the average temperature, T_{out} and T_{in} are the outlet and inlet temperature of air, respectively.

The pressure drop, ΔP between the inlet and outlet is evaluated based on Equation (3.13)

$$\Delta P = P_{in} - P_{out} \quad (3.13)$$

where P_{in} and P_{out} are the inlet and outlet pressure, respectively.

Table 3.3 Comparison of pressure drop with experimental results from Kim et al. [28] and numerical results from Mostafa et al. [27].

No.	Mass Flow Rate, \dot{m}_a (kg/s)	Pressure Drop, ΔP (Pa)				
		Simulation Results	Experimental (Kim et al. [28])	Percentage difference (%)	Numerical (Mostafa et al. [27])	Percentage Difference (%)
1	0.000981	0.769	0.997	22.861	0.733	4.997
2	0.001962	2.654	3.054	13.086	2.568	3.338
3	0.002944	5.622	5.750	2.223	5.639	0.311
4	0.003925	9.662	9.505	1.652	9.791	4.039

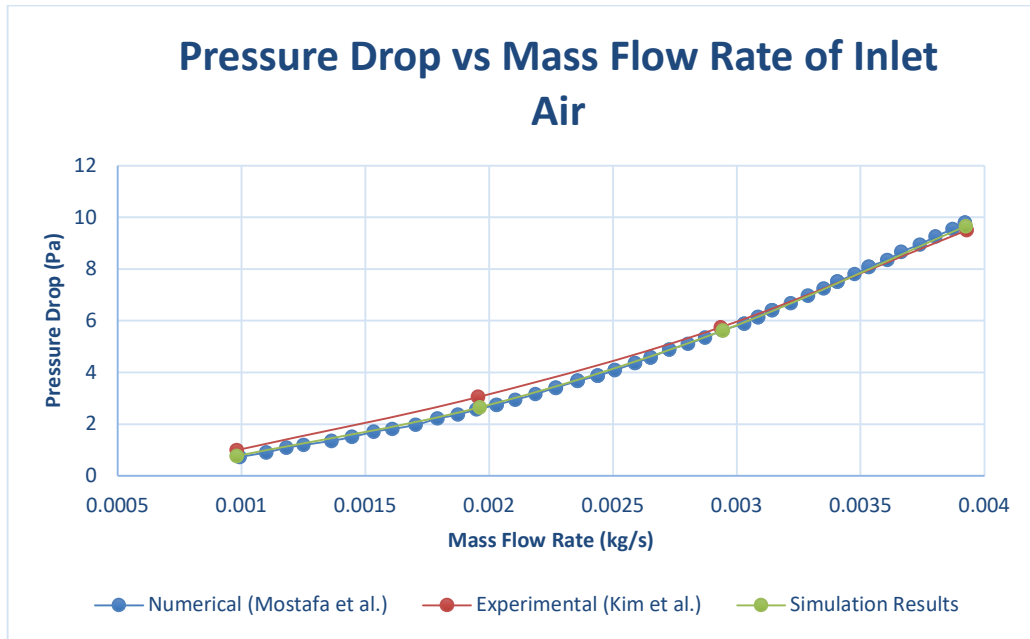


Figure 3.4 Comparison of pressure drop with experimental results from Kim et al. [28] and numerical results from Mostafa et al. [27].